The moonlighting protein c-Fos activates lipid synthesis in neurons, an activity that is critical for cellular differentiation and cortical development

Received for publication, July 10, 2019, and in revised form, April 28, 2020 Published, Papers in Press, May 8, 2020, DOI 10.1074/jbc.RA119.010129

Lucia Rodríguez-Berdini, Gabriel Orlando Ferrero, Florentyna Bustos Plonka, Andrés Mauricio Cardozo Gizzi, César Germán Prucca, Santiago Quiroga, and Beatriz Leonor Caputto*

From the Centro de Investigaciones en Química Biológica de Córdoba (Consejo Nacional de Investigaciones Científicas y Técnicas), Departamento de Química Biológica "Ranwel Caputto", Facultad de Ciencias Químicas, Universidad Nacional de Córdoba, Córdoba, Argentina

Edited by Dennis R. Voelker

Differentiation of neuronal cells is crucial for the development and function of the nervous system. This process involves high rates of membrane expansion, during which the synthesis of membrane lipids must be tightly regulated. In this work, using a variety of molecular and biochemical assays and approaches, including immunofluorescence microscopy and FRET analyses, we demonstrate that the proto-oncogene c-Fos (c-Fos) activates cytoplasmic lipid synthesis in the central nervous system and thereby supports neuronal differentiation. Specifically, in hippocampal primary cultures, blocking c-Fos expression or its activity impairs neuronal differentiation. When examining its subcellular localization, we found that c-Fos co-localizes with endoplasmic reticulum markers and strongly interacts with lipid-synthesizing enzymes, whose activities were markedly increased *in vitro* in the presence of recombinant c-Fos. Of note, the expression of c-Fos dominant-negative variants capable of blocking its lipid synthesis–activating activity impaired neuronal differentiation. Moreover, using an *in utero* electroporation model, we observed that neurons with blocked c-Fos expression or lacking its AP-1–independent activity fail to initiate cortical development. These results highlight the importance of c-Fos–mediated activation of lipid synthesis for proper nervous system development.

Neuronal differentiation, an intricate cellular process, comprises a series of complex and coordinated events, such as cell proliferation, migration, and differentiation (1–5). To reach its final structure and establish functional neuronal circuits, a neuron must promote neuritogenesis, neurite elongation, polarization, arborization, and synaptogenesis (6–8). The proper function of the nervous system heavily relies on the number of multiple and targeted synaptic contacts established by each neuron. Sprouting of axon branches along the axon shaft allows multiple innervation targets (9). The overall process of neuronal differentiation determines patterns of connectivity of neuronal circuits, whereas the disruption of these patterns may cause severe pathologies or developmental disorders (10, 11).

Outgrowth events involve cellular volume and surface area increase, thus demanding membrane material that must be supplied according to the temporal and spatial requirements of the cells in their different developmental stages (5, 6, 12–14). In fact, membrane expansion can reach an increment of up to 20% according to the different steps of neuronal differentiation (13).

Considering their architecture and size, it is reasonable to hypothesize that neurons will need temporal and domain-specific mechanisms to regulate the synthesis of the components required according to their local demands. In line with this hypothesis, Tsukita and Ishikawa (15) provided evidence of the three-dimensional structure of the endoplasmic reticulum (ER) in axonal processes. Several reports later convincingly demonstrated a synthetic machinery present in axons, with the capacity to regulate the levels of proteins, lipids, and other macromolecules (16, 17). Consequently, the mechanisms by which neurons supply components for membrane biogenesis, such as lipids in growing axons, have been the subject of several studies. Using compartmented culture systems, compelling evidence emerged demonstrating that axons carry out active lipid synthesis (18–20).

The expression of *Fos,* an oncogene of the immediate early gene family, is rapidly and transiently induced in different cell types by diverse stimuli (*i.e.* growth factors, neurotransmitters) (21–23). The proteins of the Fos family (c-Fos, Fos-B, ΔFos-B, Fra-1, Fra-2) heterodimerize mainly with those of the Jun family, comprising the well-known AP-1 transcription factors (24). Our laboratory described c-Fos as a moonlighting protein capable of achieving an additional, non-AP-1 function: it associates with the ER membranes and activates lipid synthesis through an interaction with specific lipid-synthesizing enzymes (25–31). Using PC12 cells, we distinguished between the two known functions of c-Fos (*i.e.* its AP-1 activity and its capacity to activate lipid synthesis). Initially, when cells are stimulated with nerve growth factor to differentiate into a sympathetic neuron phenotype, c-Fos is required in the nucleus to trigger the genomic program of differentiation. However, once the cells have been primed to differentiate, c-Fos is only required at the cytoplasm, associated to the ER, activating phospholipid synthesis, for cells to continue differentiating (32).

This article contains supporting information.

* For correspondence: Beatriz Leonor Caputto, bcaputto@fcq.unc.edu.ar.
Present address for Gabriel Orlando Ferrero: Centro de Investigación y Tecnología Química "Prof. Dr. Oscar A. Orio" (Consejo Nacional de Investigaciones Científicas y Técnicas), Universidad Tecnológica Nacional, Facultad Regional Córdoba, Ciudad Universitaria, Córdoba, Argentina.

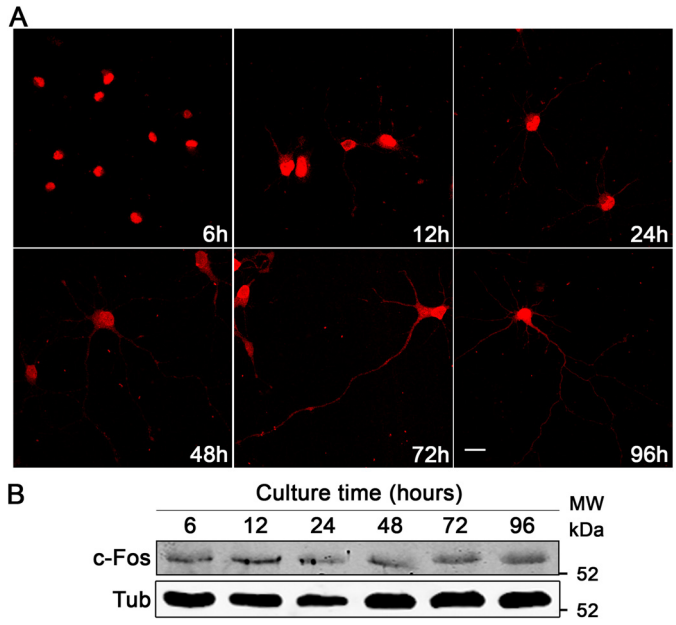

Figure 1. c-Fos is expressed in primary rat hippocampal neuronal cultures. *A*, rat primary hippocampal neurons were fixed at different times of culture and immunostained with an anti-c-Fos antibody (*red*). *Scale bar*, 20 μm. *B*, Western blotting of hippocampal cell lysates harvested at different times of culture. Membranes were immunostained with an anti c-Fos antibody (*top*) and an anti-tubulin (*Tub*) antibody (*bottom*) as a loading control and secondary antibodies suitable for near-IR fluorescence. The obtained images were converted to *gray scale* and *inverted*. The results of one of three independent experiments are shown.

Herein, using hippocampal neurons, we have shown that c-Fos is capable of exerting its lipid synthesis activator capacity in the nervous system and that this AP-1–independent activity is crucial for normal neuronal differentiation. Furthermore, by *in utero* electroporation, we demonstrate that this role is involved in cortical development. In this direction, c-Fos could be an active player in different events required for neuronal plasticity, such as those involved in learning and memory formation.

Results

c-Fos expression during neuronal differentiation

The presence of c-Fos in the brain, and more specifically in the hippocampus, was demonstrated almost 30 years ago by Dragunow *et al.* (33, 34). We initially evaluated c-Fos expression over time in primary cultures of rat hippocampal neurons. At all times examined, c-Fos was expressed at similar levels even after 96 h in culture, as determined by immunocytochemistry and Western blotting (Fig. 1). It is important to highlight that c-Fos expression is observed not only in the nucleus but also extending to the entire cytoplasm of the neurons.

We then evaluated whether c-Fos participates in the differentiation of rat hippocampal neurons. The method applied to determine the differentiation stage of the cultured cells was the one described by Dotti *et al.* (7). Briefly, cells in stage 1 of differentiation, shortly after they attach to the substrate, show motile lamellipodia developed around the periphery of the cell. At stage 2, these lamellipodia begin to transform into distinct minor processes that extend to a length of up to 10-15 μM. At stage 3, one of these minor processes begins to grow 5–10 times faster than the rest of them, indicating that the axon of the cell has been formed and the cell has polarized. At stage 4, a significant development of dendrites initiates, and finally, at differentiation stage 5, the axonal and dendritic arbors undergo a maturation process.

To evaluate the effect of blocking c-Fos activity during this complex process, primary cultures of rat hippocampal neurons were profected at 2 h of culture with anti-c-Fos antibodies or with a nonrelated antibody as a control using the BioPORTER system. Cells were examined 48 h later by immunocytochemistry but only using secondary antibodies in the case of the anti-c-Fos–profected cells. As can be seen in the graphs of Fig. 2*A*, blocking c-Fos activity impairs axon formation. We quantified different morphological features of the neurons, observing that there were no changes in soma size or in the mean number of neurites per cell when comparing cells lacking c-Fos activity and the control ones. It should be noted that we were not able to observe the development of axonal-like processes even after 48 h of culture when c-Fos activity was impaired, a phenomenon not observed in the control cells (Fig. 2*A*).

These results were confirmed by blocking c-Fos expression. When neurons were infected 2 h after seeding with lentiviral vectors designed to express a specific shRNA against c-Fos, impaired differentiation was clearly observed (Fig. 2*B*). When neurons were classified into the differentiation stages according to their morphology, more than 85% of the c-Fos-knocked-down neurons remained at stages 1 and 2 of differentiation as compared with the almost 50% of neurons in stages 3 and 4 of the control cultures (Fig. 2*C*).

c-Fos co-localizes with ER markers in neuronal processes

Previous studies from our laboratory have shown that upon a subcellular fractionation of PC12 cell homogenates, c-Fos and the ER membranes are predominantly collected in the same fraction (35). This led us to examine whether the c-Fos/ER co-localization observed previously can be evidenced in neurons of the central nervous system as well. To test this, we performed immunocytochemistry assays on primary rat hippocampal neurons after 48 h of culture, and, as expected, a strong co-localization of c-Fos with the ER marker calnexin was detected (Fig. 3). Surprisingly, c-Fos and the ER were found not only in the perinuclear region of the soma; defined co-localization dots at punctuate structures confined to axonal branching points were also very frequently observed.

c-Fos activation of lipid-synthesizing enzymes in neurons

Previous results from our group have demonstrated that c-Fos physically interacts with and activates particular enzymes of the lipid synthesis pathways. Such is the case for CDP-diacylglycerol synthase (CDS), PI4KIIα (phosphatidylinositol 4 kinase II-α), and Lipin1 (29, 31). Taking this into consideration, it was hypothesized that c-Fos could be involved in neuronal differentiation by a lipid-activating mechanism that requires its physical interaction with specific enzymes. To this end, we examined the possible interaction of c-Fos with CDS, the enzyme that catalyzes the conversion of phosphatidic acid into CDP-diacylglycerol (CDP-DAG), the first step of phosphatidylinositol-phosphate synthesis in the ER. To infer protein-

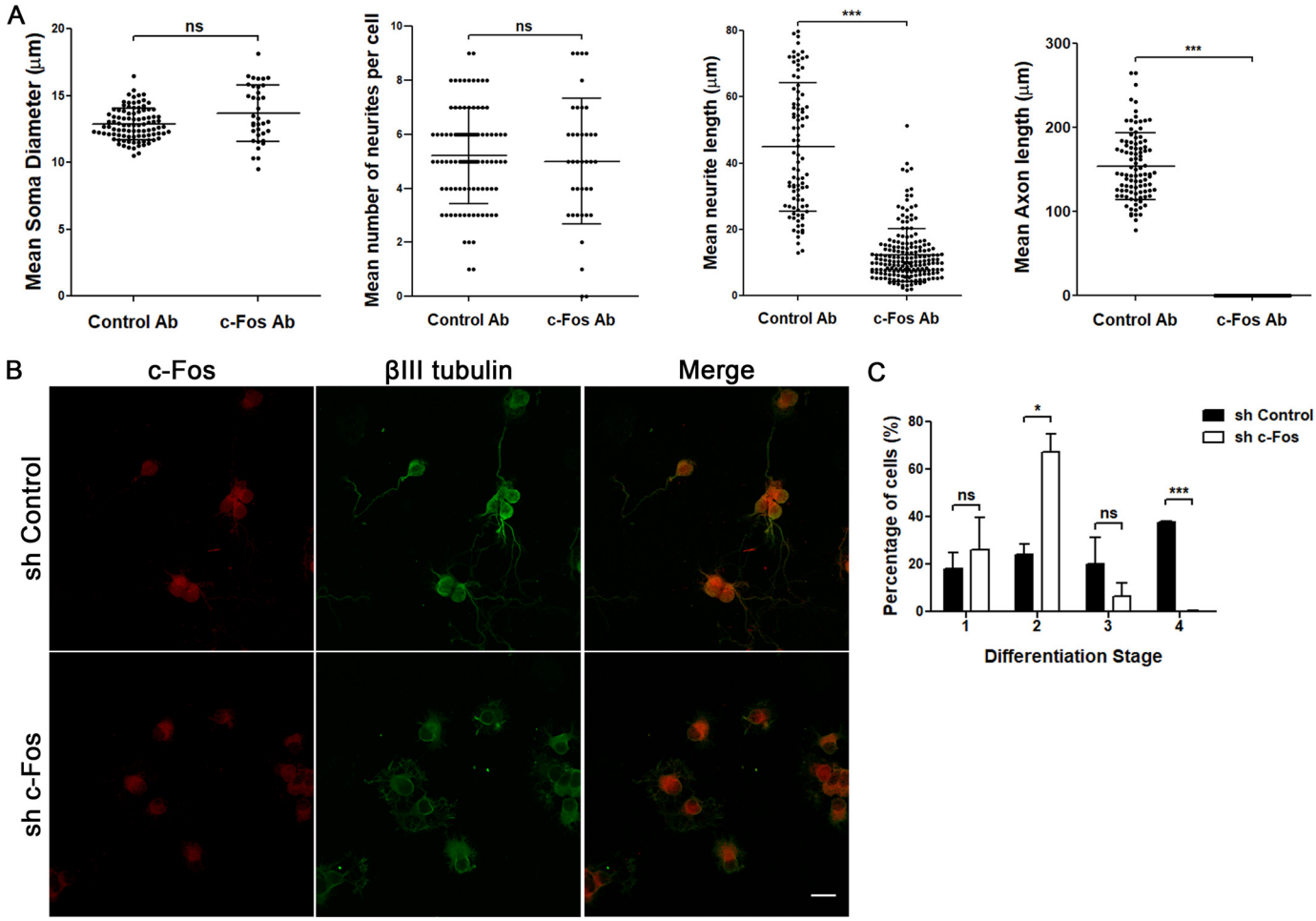

Figure 2. Blocking the activity or the expression of c-Fos impairs neuronal differentiation. *A*, cells were profected with anti c-Fos (c-Fos Ab) or with a nonrelated anti-mouse IgG antibody as a control (*Control Ab*) 2 h after seeding using BioPORTER and then were fixed after 48 h of culture. The different morphological aspects were quantified from microscopy images, using ImageJ software, and are shown as the mean ± S.D. (*error bars*) in each case. Student's *t* test statistical analysis was performed using GraphPad Software. ***, $p < 0.001$; *n.s.*, nonsignificant; in each experiment, $n = 40$ cells from each condition were examined. Results of one of three independent experiments performed are shown. *B*, cells were infected at the initiation of the culture with lentiviral particles designed to express an anti c-Fos shRNA or an shRNA with a scrambled sequence of c-Fos as a control. After 48 h of culture, cells were fixed and immunostained with an anti-c-Fos antibody (*red*, *first column*) and an anti βIII-tubulin antibody (*green*, *second column*). The *third column* shows the merge between both labels. *Scale bar*, 20 μm. *C*, morphological quantification of neuronal differentiation stages in both c-Fos and scrambled infected cells was performed using ImageJ software. The graph shows the mean number of cells ± S.D. in each case. Student's *t* test statistical analysis was performed using GraphPad software. *, $p < 0.05$; ***, $p < 0.001$; *n.s.*, nonsignificant; $n = 198$ cells for scrambled shRNA–infected cells, $n = 254$ cells for c-Fos shRNA-infected cells. Results of one of three independent experiments performed are shown.

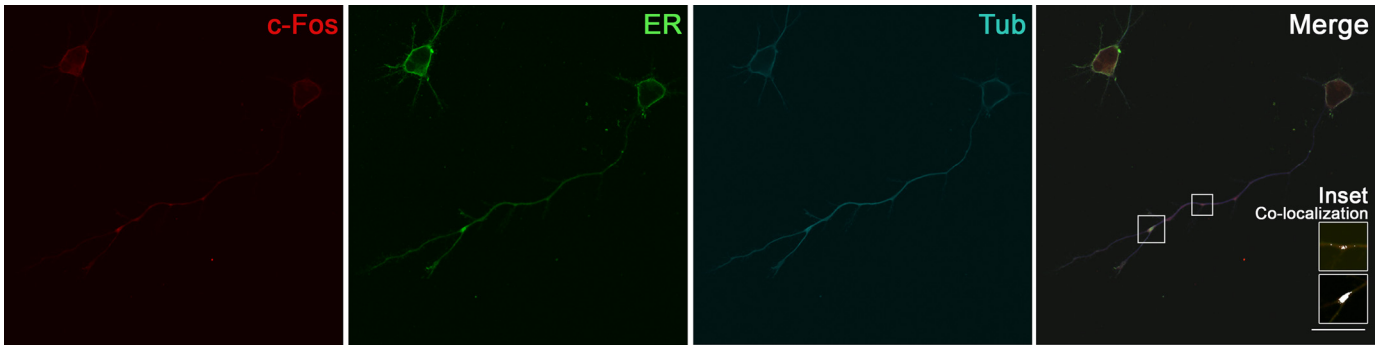

Figure 3. c-Fos co-localizes with ER markers. Immunocytochemistry of c-Fos (*red*), the ER marker calnexin (*green*), and βIII-tubulin (*cyan*) of rat hippocampal neurons at 48 h of culture. The *fourth panel* shows the merged images between the three labels. A Pearson's *r* value of 0.81 was calculated for co-localization of both labels (Coloc2, ImageJ). An *inset* is shown with a co-localization analysis between c-Fos and the ER, where the co-localizing pixels are *colored* in *white* (Colocalization Finder, ImageJ). *Scale bar*, 20 μm. The results of one of three independent experiments are shown.

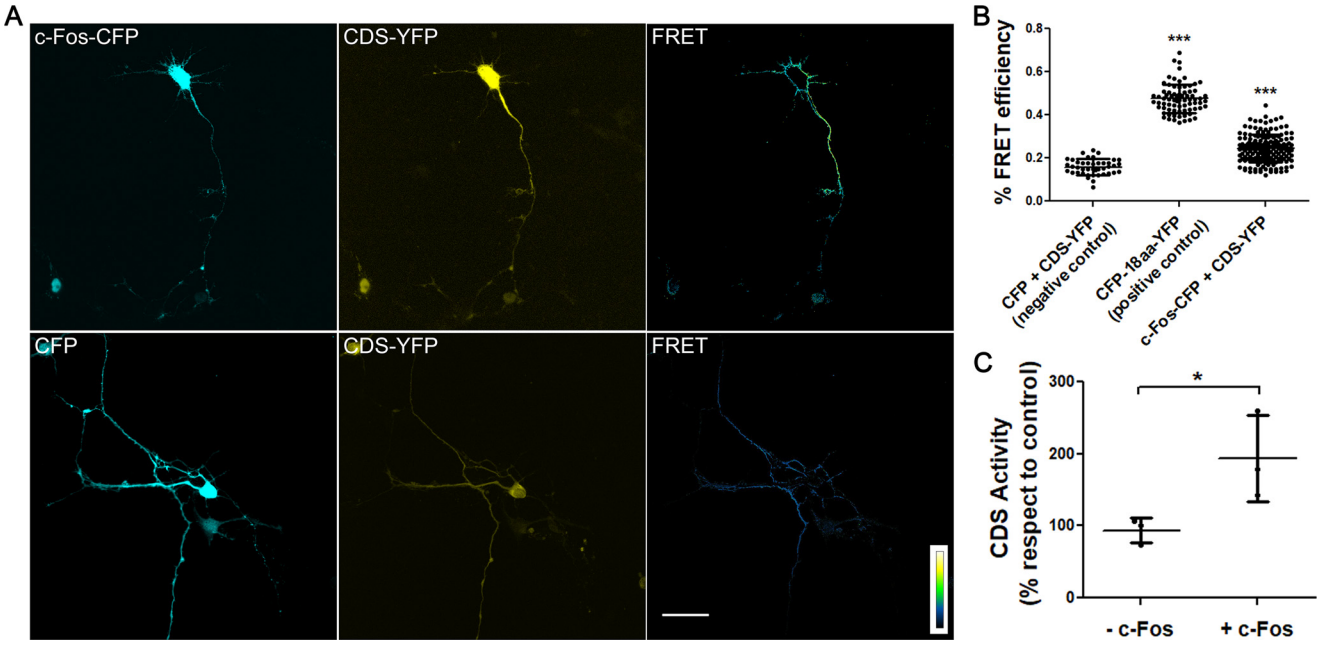

Figure 4. c-Fos activates and physically interacts with CDS. *A, top row*, neurons were co-transfected at 24 h of culture to express c-Fos-CFP (*first panel*) and CDS-YFP (*second panel*) and examined by confocal microscopy at 48 h. FRET images were obtained by the sensitized emission method and *pseudocolored* using ImageJ software (*third panel*). The *bottom row* shows a negative control with cells co-transfected with the CFP empty vector and CDS-YFP. The *scale* goes from no FRET (*black*) to maximum FRET (*yellow*). *Scale bar*, 30 μm. *B*, the graphic shows the quantification of the mean efficiencies ± S.D. (*error bars*) for the donor/acceptor pairs shown in the images, with one-way ANOVA and Tukey's post-test. ***, $p < 0.001$; $n = 25$ cells for each condition. The results of one of three independent experiments are shown. *C*, evaluation of CDS activity through measurement of the incorporation of [^{3}H]CTP into CDP-DAG in neuron homogenates in the presence of c-Fos (+ *c-Fos*). Elution buffer was used as a control (– *c-Fos*). Results are the mean of three independent experiments performed in triplicate. The results are expressed as the mean ± S.D., with Student's *t* test analysis. *, $p < 0.05$.

protein interactions, FRET experiments were performed (36). For this, rat primary hippocampal neurons were co-transfected to express c-Fos-mTurquoise2 and CDS-SYFP2 and examined by confocal microscopy. As shown in Fig. 4 (*A* and *B*), a positive FRET phenomenon is observed between both proteins, indicating that there is indeed a physical interaction between them.

To study whether this physical interaction leads to enzyme activation, CDS activity was assayed using cell homogenates obtained from rat hippocampal neurons as the enzyme source and [^{3}H]CTP and dioleoyl-phosphatidic acid as substrates, with or without the addition of recombinant c-Fos to the incubates (29, 37, 38). At the times assayed, about 40% more CDP-DAG was synthetized in the +c-Fos incubates as compared with the control (Fig. 4*C*). This confirms that the lipid synthesis activation mediated by c-Fos observed previously also occurs in hippocampal neurons in culture. The association of c-Fos with CTP:phosphocholine cytidylyltransferase (CCT), the rate-limiting enzyme in phosphatidylcholine synthesis (Fig. S1), suggests that c-Fos could be also mediating the activation of other phospholipid pathways.

Neuronal differentiation is impaired in cells lacking cytoplasmic c-Fos

The results shown so far support the need of c-Fos to normally complete the differentiation events. However, they do not allow us to discern whether the effect is due to the AP-1 or the lipid synthesis activator function of c-Fos. To activate lipid synthesis, c-Fos associates through its N-terminal domain (NA domain, amino acids 1-138 of full-length c-Fos) with the enzymes it activates (29, 31, 32). However, this portion of the protein is not sufficient to produce lipid synthesis activation because of the absence of the basic domain (BD, amino acids 139-159), a domain required for enzyme activation to occur. As the NA domain is not involved in c-Fos AP-1 functions, it seems reasonable to propose its use as a dominant negative of its lipid synthesis activator function. In other words, the NA should interfere only with the lipid-synthesizing function of c-Fos and not with its AP-1, transcriptional one. Furthermore, we have previously shown that recombinant NA is not able to activate total phospholipid synthesis and inhibits CDS activity (30, 38).

Taking this into consideration, we examined whether the impairment in neuronal differentiation could be linked to the lack of c-Fos–dependent lipid synthesis activity. Hippocampal neuronal cells were transfected with a construct that contains the NA domain, which does not activate lipid synthesis, or with the construct NB, which contains amino acids 1–159 (NB domain), which is capable of activating lipid synthesis at levels comparable with those of full-length c-Fos, both fused with YFP. The empty vector was used as a control. Then the differentiation stages of the transfected cells at different fixation times were analyzed. It can be seen in Fig. 5*A* and its quantification in Fig. 5*B* (cells fixed at 48 h) that the expression of the NA domain impairs neuronal differentiation as evidenced after a morphological analysis and stage quantification of the NA-transfected cells relative to the NB-transfected or nontransfected ones. Even more, it is clear that the impairment in differentiation promoted by the NA domain is comparable with that observed when c-Fos expression is blocked (Fig. 2, *B* and *C*).

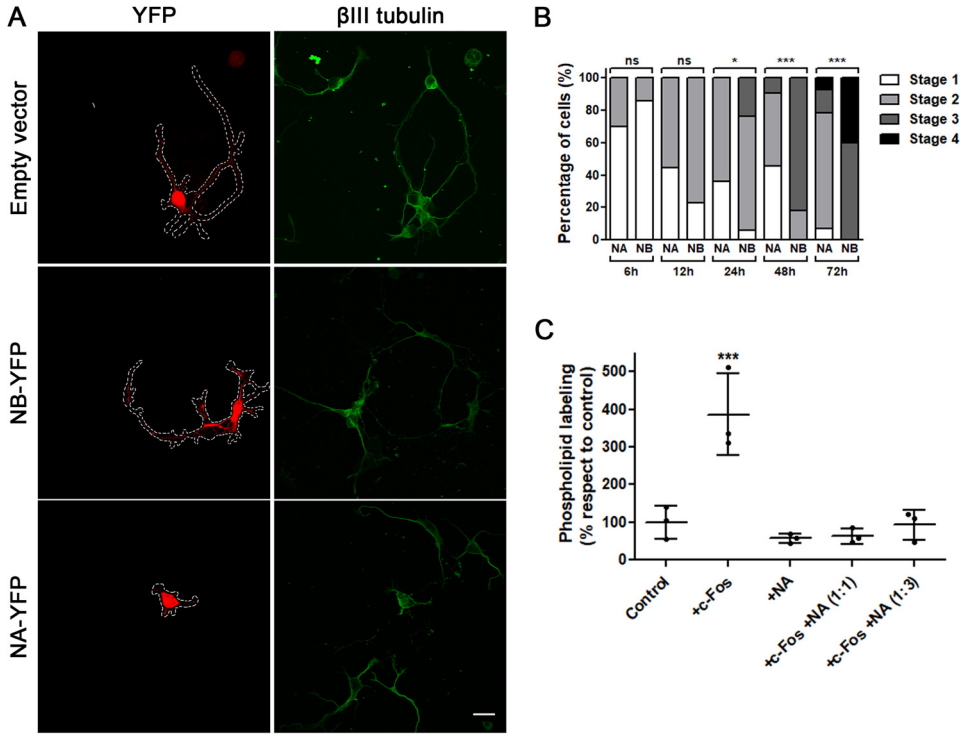

Figure 5. NA deletion mutant of c-Fos impairs differentiation in neuronal cultures and abrogates c-Fos-dependent lipid synthesis activation. *A*, neuronal cultures were transfected at seeding with NA-YFP (*pseudocolored red*, *bottom row*), NB-YFP (*pseudocolored red*, *middle row*), or the empty vector as a control (*pseudocolored red*, *top row*) and were fixed after 48 h of culture. Cells were subjected to immunofluorescence against βIII-tubulin (*green*, *second column*). *Scale bar*, 20 μm. *B*, morphological quantification of neuronal differentiation stages in both NA-YFP– and NB-YFP–transfected cells at different fixation times. The results of one of three independent experiments are shown. A normality Kolmogorov–Smirnov test was performed, where the deviation from the distribution with respect to the NB-transfected cells was evaluated. *, $p < 0.05$; ***, $p < 0.001$; *n.s.*, nonsignificant; $n = 15$ from each condition were examined. *C*, evaluation of ^{32}P-phospholipid labeling capacity of neuron homogenates in the presence of c-Fos (+*c-Fos*), NA (+*NA*), or both (+*c-Fos* +*NA 1:1* and +*c-Fos* +*NA 1:3*). Elution buffer was used as a control (*Control*). Results are the mean of three independent experiments performed in triplicate. The results are expressed as the mean ± S.D. (*error bars*), with one-way ANOVA. ***, $p < 0.001$ with respect to control conditions.

To test whether this effect was due to the lipid synthesis activator capacity of c-Fos, we performed biochemical assays to assess total phospholipid labeling in homogenates obtained from hippocampal neurons primary cultures. Previous reports have shown that the γ-phosphate group of labeled [^{32}P]ATP can be incorporated into different lipids of cell lysates assayed *in vitro*, mainly phosphatidylinositol and its derivatives and phosphatidic acid (39–44), and that recombinant c-Fos promotes an increase in their synthesis (45). When assaying this in neurons, it is clear that the addition of recombinant c-Fos to the assay promotes a significant increase in total phospholipid labeling, whereas recombinant NA does not (Fig. 5*C*). However, if both c-Fos and NA are added together, the activating effect of c-Fos is abolished. These results are compatible with a competition between c-Fos and NA for binding of c-Fos to the enzymes as shown previously in other systems (38). This is also compatible with the notion that differentiation is impaired as a consequence of the lack of the lipid synthesis activator capacity of c-Fos.

c-Fos is essential for cortical development

We next studied whether c-Fos participates in cortical development *in vivo* by using *in utero* electroporation. Briefly, the vertebrate cortex is organized into layers of neurons that share functions, morphology, and birthdates (46). During development, radial glia progenitors in the ventricular zone (VZ) divide asymmetrically to originate cortical pyramidal projecting neurons. Then they suffer a radial migration process toward the marginal zone and through the subventricular zone (SVZ) and lower intermediate zone (IZ). In the IZ, neurons acquire a transient multipolar morphology where they extend and retract multiple dynamic projections and move in apparently random directions (47–49). As cells approach the middle of the IZ, the genesis of the axon starts, and when they reach the upper region of the IZ, they change their morphology from multipolar to bipolar and carry on radial migration (46, 50, 51).

Using the electroporation model, it can be determined whether the manipulated neurons, which are destined to migrate to the upper layers of the brain cortex, suffer an impairment in this process or in the establishment of neuronal polarity. Cortical progenitors at embryonic day 15 (E15) were electroporated with a specific shRNA targeting c-Fos, and an analysis of the location and morphology of the progeny was performed at E19 after *in vivo* differentiation. Visualization of the electroporated cells was achieved by co-electroporating the shRNAs with a plasmid encoding the DsRed fluorescent protein.

We first analyzed differentiation of cells electroporated with a nonrelevant shRNA (shControl) plus DsRed at E19. About 10% of the neurons were located in the VZ/SVZ, 30% of cells were found migrating through the IZ, and the majority (60%) had reached the top of the cortical plate (Fig. 6*A* (*left*);

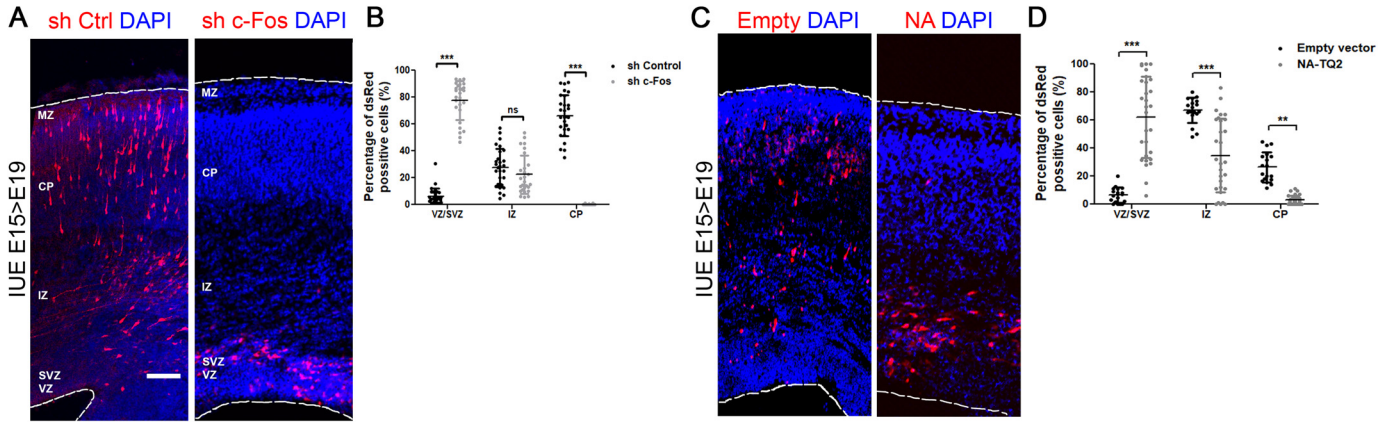

Figure 6. Expression of c-Fos is involved in cortical development. *A*, embryo brains were electroporated with a specifically designed shRNA to block c-Fos expression (*sh c-Fos*) (*right*) or a control scrambled shRNA (*left*) at E15 and analyzed at E19. *IUE, in utero* electroporation; *MZ*, marginal zone. *Scale bar*, 100 μm. *B*, quantification of the distribution of dsRed-positive cells in the CP, IZ, and VZ/SVZ. The mean ± S.D. of the quantification of at least 20 coronal cryosections from three independent experiments performed independently is shown, with two-way ANOVA with Bonferroni post-test. ***, $p < 0.001$; *n.s.*, nonsignificant. *C*, embryo brains were electroporated with a vector designed to express the NA domain of c-Fos fused to CFP or the empty vector as a control at E15 and analyzed at E19. *D*, quantification of the distribution of dsRed-positive cells in the CP, IZ, and VZ/SVZ. The mean ± S.D. of the quantification of at least 20 coronal cryosections from three independent experiments performed independently is shown, with two-way ANOVA with Bonferroni post-test. ***, $p < 0.001$; **, $p < 0.001$.

quantification in Fig. 6*B*). Cells with knocked-down expression of c-Fos clearly showed an altered distribution and abnormal migration: around 80% of the cells remained arrested at the VZ/SVZ compared with the 10% in this localization in control experiments, and practically no electroporated cells were observed in the upper cortical plate (CP) (Fig. 6*A* (*right*); quantification in Fig. 6*B*).

Electroporation assays were then performed with the deletion mutants of c-Fos to evaluate whether its lipid synthesis activator function is responsible for the abnormal phenotype observed when c-Fos expression is blocked. Electroporated cells of control experiments using the empty vector show a localization similar to that shown in the controls of Fig. 6*A* (Fig. 6*C* (*left*); quantification in Fig. 6*D*). By contrast, cells transfected with c-Fos NA domain, which acts as a dominant negative of its lipid synthesis activator function, remained arrested at the VZ/SVZ and IZ (Fig. 6*C* (*right*); quantification in Fig. 6*D*). These results support the notion that the AP-1–independent function of c-Fos is in fact involved in cortical development.

Discussion

Although for a long time it was assumed that biosynthesis of most macromolecules in neurons was confined to the cell body (52, 53), an increasing body of molecular evidence has supported the presence of functional ER-resident components in axons (15–17, 54–62). Together with the understanding of the complex structural features of the axonal ER, different studies provided emerging evidence of active, axon-localized lipid synthesis (18, 19, 63–66). In fact, in the case of phosphatidylcholine synthesis, almost 50% has been found to be locally synthesized in distal axons, and it is required for axonal growth (20). Although this highlights the importance of the axonal ER in lipid homeostasis and in the maintenance of the complex structure of neurons, there have been no significant advances in recent years regarding the regulation of lipid metabolism in neurons.

Taking into consideration that the plasma membrane surface area of a developing neuron increases up to 20% per day (13) and that the compositional differences along the membrane due to the functional differences of axons and dendrites must necessarily be maintained, the molecular mechanisms regulating localized lipid synthesis must be carefully orchestrated. Because most of the local metabolic demands for axonal development, plasticity, or regeneration must be rapidly supplied, it seems reasonable to propose that, at least in part, the mechanisms involved in lipid synthesis regulation could be independent of the cells' nuclear activity. In the present work, we provide evidence that confirms the existence of the AP-1–independent function of c-Fos as a lipid synthesis activator in the nervous system, particularly in rat hippocampal neurons in culture and in the developing brain cortex during embryonic stages.

The fact that c-Fos is expressed during neuronal differentiation but is not in the adult brain in nonpathological conditions (67) implies that its expression is related to developmental events. c-Fos was described as a marker of neuronal activity, specially tied to learning and memory processes (68). In the experiments presented herein where c-Fos expression or its activity is blocked, neurons do not develop an axon and remain at early stages of differentiation without a distinguishable axon even after 48 h of culture. Until now, the effects of c-Fos on neuronal plasticity have always been linked to gene expression through its nuclear function, but given the evidence presented herein, it is possible that they are associated with processes that involve changes in lipid homeostasis. This can be particularly visualized in the experiments carried out with dominant negative of the lipid synthesis activator function of c-Fos, where the same results of impairment on differentiation in culture are observed although AP-1 activity should not be affected.

This hypothesis can be extended to cortical development: when performing *in utero* experiments, the cells with no c-Fos expression remain at the ventricular and subventricular zones instead of migrating to the superior layers of the cortex, an observation that implies a strong failure in normal cortical

development. These results deepen our previous findings in the cerebral cortex of *fos* (−/−) mice, which show a strong reduction in the cortex thickness and a marked tendency of cells toward an undifferentiated phenotype (69). Because the *in utero* model does not have compensatory effects relying on other proteins that might fulfill the function of c-Fos, the phenotype observed in our experiments confirms the importance of this protein in cortex development. Even more, the same *in utero* experiments with dominant negatives of its AP-1–independent function show that this effect is directly related to its lipid synthesis activator role. However, the changes in the localization of the NA-transfected cells are not as extreme as those observed in the c-Fos-knocked-down cells. Two different interpretations arise from the intermediate phenotype observed in this case: both functions, AP-1 and lipid synthesis activation, are actively involved in cortical development, or the expression level of the NA domain is not enough to displace all of the endogenous c-Fos molecules. It remains to be determined whether the observed phenotype is a consequence of failures in polarization or migration of the cells.

c-Fos has been implicated in numerous physiological processes in the nervous system. It was the first transcription factor whose induction was proven to be dependent on the activity of the neuron (70, 71), a finding that rapidly transformed c-Fos in a marker of neuronal activity. In fact, it has been consistently demonstrated that its expression rises in the central nervous system after learning or memory trainings (68), although these changes are observed only during the first sessions of the protocols, indicating that this is probably an adaptive response. Given the results presented in this work, it seems reasonable to hypothesize that c-Fos lipid activator function could be involved in processes related to neuronal plasticity and learning processes by providing new membrane lipids for the establishment of new circuits that are no longer required once they are formed.

In light of all of the above-mentioned results, the role of AP-1–independent c-Fos is of vital importance for neuronal development. Its lipid synthesis activator capacity might contribute to the high membrane expansion rates necessary for the extension of the different neuronal processes that favor polarization and the correct establishment of synaptic connections for normal nervous system function.

Experimental procedures

Cell cultures, profection, and transfection

Dissociated hippocampal pyramidal neurons were prepared from fetal rat brain and cultured as described (72). Briefly, pregnant *Rattus norvegicus* Wistar rats at 18 days postfertilization were euthanized, and prenatal pups were excised from the uterus with sterile dissecting scissors. Pups were then decapitated with sterile scissors in a laminar flow hood, and the removed heads were placed in plates with sterile Hanks' balanced salt solution (Sigma–Aldrich) at 4 °C under a dissecting microscope. After hippocampus isolation and dissociation with 0.25% trypsin (Thermo Fisher Scientific), the tissue was dissociated with Pasteur pipettes. The cells obtained were plated onto acid-washed, polylysine-coated glass coverslips or polylysine-coated plates and maintained in Dulbecco's modified Eagle's medium (Thermo Fisher Scientific) supplemented with 10% (v/v) horse serum (Thermo Fisher Scientific) for 2 h, after which the culture medium was replaced with serum-free Neurobasal medium supplemented with N2 and B27 supplements (Thermo Fisher Scientific). Cultures were maintained in a humidified 37 °C incubator with 5% CO_2 for the indicated times.

Profections were performed using BioPORTER® Protein Delivery Reagent (Genlantis, San Diego, CA, USA) and transfections using Lipofectamine 2000 (Thermo Fisher Scientific) according to the manufacturer's protocol.

Production of shRNA containing lentiviral particles

Upon desired confluence, embryonic kidney epithelial HEK 293T cells (ATCC, Manassas, VA, USA) were co-transfected with MISSION® c-Fos custom shRNA plasmids (clones ID TRCN0000042680 and TRCN0000042678) cloned in pLKO.1-CMV-tGFP (Sigma–Aldrich) or with the control scrambled shRNA sequence and with compatible packaging plasmids using Lipofectamine 2000 (Thermo Fisher Scientific). Lentiviral titer was determined according to the manufacturer's protocol (MISSION®, Sigma–Aldrich).

Preparation of recombinant c-Fos and NA

His-tagged c-Fos and NA were expressed and recovered from pDS56-HisFos–transformed BL21 cells as described previously (30, 38, 73).

Co-immunoprecipitation assays, electrophoresis, and Western blotting (WB)

For co-immunoprecipitation assays, 500 μg of total protein from cells treated as indicated were immunoprecipitated for 4 h at 4 °C with Protein G–Sepharose (GE Healthcare) with the desired antibody and washed, and immunodetection was performed as described below. Cell lysates (50 μg) or immunoprecipitates were fractionated through SDS-containing polyacrylamide gels (12%) and electrotransferred to a nitrocellulose membrane at 300 mA for 1 h. Immunodetection was carried out by blocking of membranes with 10 mM PBS containing 5% (w/v) nonfat dried milk for 1 h at RT, followed by incubation with the desired antibody overnight at 4 °C in PBS-0.1% (v/v) Tween 20 (Sigma–Aldrich). Membranes were washed three times (10 min) with PBS-0.1% (v/v) Tween 20 and incubated for 1 h at RT with secondary antibodies. Membranes were washed, and detection was performed using an ODYSSEY IR imaging system (LI-COR, Lincoln, NE, USA).

In vitro phospholipid labeling

In vitro phospholipid labeling capacity of neurons was assayed as described previously (32, 74). Briefly, reactions were incubated for 60 min at 37 °C in a final volume of 50 μl containing 50 μg of cell homogenate protein as the enzyme source, 2.8 mM NaCl, 100 mM KCl, 10 mM $MgCl_2$, 112 mM glucose, HEPES buffer, pH 7.5, 1.5 μCi of [^{32}P]ATP (specific activity 3000 Ci/mmol; PerkinElmer Life Sciences) and the indicated amounts of c-Fos or NA. Conditions of linearity with time and protein

concentration were determined for the enzyme with 1 ng of recombinant proteins per μg of protein cell homogenate, suspended in 3 μl of elution buffer or an equal volume of elution buffer for control reactions. For the competition conditions, the ratios between c-Fos and NA were calculated according to the number of molecules of each protein. Reactions were stopped by the addition of TCA and phosphotungstic acid (PTA; 5:0.5% (w/v), respectively). Incubates were centrifuged, and the pellet was washed three more times with TCA-PTA, 5:0.5% (w/v). After a final washing step with water, the pellet was suspended in 1.5 ml of chloroform/methanol (2:1). In this phase partitioning, lipids remain in the organic phase. Phospholipid labeling was quantified in the organic phase by scintillation counting (30, 74, 75). A more detailed version of the protocol has been published (76).

Enzyme activity determinations

Total CDS activity was assayed as described by Lykidis *et al.* (37). All reactions were performed in an 80-μl final volume containing 100 μg of cell homogenate protein as the enzyme source, 0.69 μM [^{3}H]CTP (PerkinElmer Life Sciences), and 2 mM phosphatidic acid (Avanti Polar Lipids, Alabaster, AL, USA). Conditions of linearity with time and protein concentration were determined for the enzyme with 0.5 ng of recombinant c-Fos per μg of protein cell homogenate, suspended in 3 μl of elution buffer or an equal volume of elution buffer for control reactions (29, 38). The reaction was started by the addition of 10 mM $MgCl_2$, and assays were incubated at 37 °C for 1 h. Reactions were stopped by the addition of 180 μl of chloroform/methanol/HCl (1:2:0.02%, v/v/v). After the addition of 60 μl of chloroform and 60 μl of KCl (2 M), phases were separated by centrifugation. The amount of [^{3}H]CDP-diacylglycerol synthesized was determined by liquid scintillation counting in the organic phase.

Immunofluorescence (IF) and microscopy

Cells grown on round, acid-washed coverslips were rinsed twice with ice-cold 10 mM PBS and fixed in *para*-formaldehyde 4% (w/v) (Sigma–Aldrich), sucrose 4% (w/v) (Sigma–Aldrich) in 10 mM PBS at 37 °C for 10 min. Cells were then permeabilized with Triton X-100 (0.1% (v/v)) (Sigma–Aldrich) in 10 mM PBS for 10 min and blocked with horse serum (2%, v/v) and bovine serum albumin (3%, w/v) in 10 mM PBS for 2 h at RT in a humid chamber. Samples were incubated overnight at 4 °C in blocking buffer containing the desired antibody, washed twice with 10 mM PBS, and incubated with secondary antibodies for 2 h at RT, washed, and mounted with FluorSave (Millipore, Burlington, MA, USA). When indicated, 4′,6-diamino-2-phenylindole, dihydrochloride (DAPI; Thermo Fisher Scientific) was used to visualize nuclear structures.

Antibodies

The following primary antibodies were used: rabbit polyclonal anti-c-Fos antibody (Santa Cruz Biotechnology, Inc., Dallas, TX, USA) diluted 1:200 for IF; rabbit polyclonal anti-c-Fos antibody (Sigma–Aldrich) diluted 1:2000 for WB; mouse monoclonal anti-α-tubulin antibody (Sigma–Aldrich) diluted 1:3000 for WB; mouse monoclonal anti-βIII-tubulin antibody (Sigma–Aldrich) diluted 1:1500 for IF; goat polyclonal anti-calnexin antibody (ER marker, Abcam, Cambridge, UK) diluted 1:500 for IF; rabbit polyclonal anti-CCTβ2 antibody (Sigma–Aldrich) diluted 1:500 for IF. The following secondary antibodies were used: IRDye 800CW goat anti-mouse antibody and IRDye 800 goat anti-rabbit antibody (LI-COR) diluted 1:25,000 for WB; Alexa 488, Alexa 546, and Alexa 633 (Thermo Fisher Scientific) diluted 1:1000 for IF.

FRET analysis

Cells grown on round, acid-washed coverslips in 24 multiwell plates were transfected with c-Fos-mTurquoise2-N1, CDS-pSYFP2, CCTβ2-pSYFP2, pSYFP2-mTurquoise2, or the empty vectors using Lipofectamine 2000 according to the manufacturer's protocol. After 24 h of transfection, cells were rinsed twice with ice-cold 10 mM PBS and fixed in *para*-formaldehyde 4% (w/v) (Sigma–Aldrich), sucrose (4%, w/v) (Sigma–Aldrich) in 10 mM PBS at 37 °C for 10 min. Cells were then washed three times with PBS and rinsed with Milli-Q water. Coverslips were mounted with FluorSave (Millipore, Burlington, MA, USA), and cells were visualized using an Olympus FV1000 laser-scanning confocal microscope with Olympus Fluoview Software (Olympus, Shinjuku, Tokyo, Japan). For FRET determinations, the sensitized emission measurement approach was used (36). The mTurquoise (donor) and SYFP (acceptor) chimeric proteins were excited with an argon laser at 458 and 515 nm, respectively. The emission channel was 470–500 nm for the donor and 530–560 nm for the acceptor. Background values were determined independently for each channel from a coverslip with nontransfected cells and then subtracted using ImageJ software. Donor spectral bleed-through and acceptor cross-excitation were calculated and corrected from single transfected cells. Mean FRET efficiency values (%E) within a cell were obtained on a pixel-by-pixel basis (31). The resulting image was then pseudocolored to better illustrate the distribution of the calculated efficiencies in the cell.

In utero electroporation

In utero electroporation was performed as described previously (77) with minor modifications. Briefly, pregnant C57BL/6J mice at E15 days were anesthetized with ketamine/xylazine (Laboratorios Richmond, Ciudad Autónoma de Buenos Aires, Argentina). Needles for injections were pulled from P-97 Flaming/Brownglass capillaries (World Precision Instruments, Sarasota, FF, USA). shRNA solutions were mixed with trypan blue 1% (v/v) at a DNA concentration of 0.5–1.5 μg/μl for each construct and injected. Five pulses of 40 V (50 ms ON, 950 OFF) were applied using 5-mm electrodes and a specially manufactured electroporator (LIADE National University of Córdoba, Córdoba, Argentina). The embryos were placed back into the abdominal cavity, which was then sutured. 3 days after intervention, the mother was sacrificed by cortical dislocation, the embryos were removed, and the brains of the electroporated ones were extracted and fixed with 4% (w/v) *para*-formaldehyde (Sigma–Aldrich) for 24 h. Then they were cryoprotected by immersion in sucrose (30%, w/v) (Sigma–Aldrich) and

finally embedded in medium for frozen tissue specimens to ensure optimal cutting temperature (O.C.T.) and frozen in nitrogen. After 3 days at −80 °C, coronal cryosections of 20 μm were obtained and processed for immunofluorescence.

Microscope image acquisition

Imaging was performed on an Olympus FV1000 laser-scanning confocal microscope using Olympus Fluoview software (Olympus, Shinjuku, Tokyo, Japan) and a ×60 (1.4 NA) oil objective or a ×10 (0.40 NA) air objective. Images were analyzed with ImageJ software.

Experimental design and statistical analysis

All of the statistical analyses were performed using GraphPad Prism software. Statistical significance was defined by a p value of <0.05. The statistical test performed and the number of replicates for each experiment are indicated in the corresponding figure legends.

Animal care

All of the procedures were performed according to the *Guide for the Care and Use of Laboratory Animals* (8th Edition) and the approved protocols of the Institutional Board for Animal Welfare (CICUAL, Facultad de Ciencias Químicas, Universidad Nacional de Córdoba, Argentina).

Data availability

All data are contained within the article.

Acknowledgments—We thank Dr. Hugo Maccioni (CIQUIBIC, CONICET, Facultad de Ciencias Químicas, Universidad Nacional de Córdoba, Argentina) for helpful discussions and critical reading of the manuscript. We greatly acknowledge the technical and imaging assistance of Dr. María Cecilia Sampedro and Dr. Carlos Rubén Más from the Centro de Micro y Nanoscopía de Córdoba, CEMINCO (CONICET), Universidad Nacional de Córdoba, Córdoba, Argentina and the technical assistance with animal care and maintenance of Elvira Rosa Andrada (CIQUIBIC, CONICET).

Author contributions—L. R.-B., G. O. F., F. B. P., S. Q., and B. L. C. conceptualization; L. R.-B., G. O. F., F. B. P., A. M. C. G., and C. G. P. data curation; L. R.-B. software; L. R.-B., G. O. F., F. B. P., A. M. C. G., and C. G. P. formal analysis; L.R .-B. validation; L. R.-B., G. O. F., F. B. P., A. M. C. G., and C. G. P. investigation; L. R.-B., G. O. F., F. B. P., A. M. C. G., and C. G. P. visualization; L. R.-B., G. O. F., F. B. P., A. M. C. G., and C. G. P. methodology; L. R.-B. and B. L. C. writing-original draft; L. R.-B., G. O. F., F. B. P., A. M. C. G., C. G. P., S. Q., and B. L. C. writing-review and editing; S. Q. and B. L. C. resources; S. Q. and B. L. C. funding acquisition; B. L. C. supervision; B. L. C. project administration.

Funding and additional information—This work was supported by the Secretaría de Ciencia y Técnica, Universidad Nacional de Córdoba; the Fondo para la Investigación Científica y Tecnológica, Ministerio de Ciencia, Tecnología e Innovación, Argentina (Grants PICT 2017-2761, PICT 2012-2797, PICT 2013-2996, and PICT 2015-3702); and the Instituto Nacional del Cáncer, Ministerio de Salud, Argentina. Gabriel Orlando Ferrero, César Germán Prucca, Santiago Quiroga, and Beatriz Leonor Caputto are members of and Lucía Rodríguez Berdini, Florentyna Bustos Plonka, and Andrés Mauricio Cardozo Gizzi are fellows of CONICET (Consejo Nacional de Investigaciones Científicas y Tecnológicas), Ministerio de Ciencia, Tecnología e Innovación, Argentina.

Conflict of interest—The authors declare that they have no conflicts of interest with the contents of this article.

Abbreviations—The abbreviations used are: ER, endoplasmic reticulum; CCT, CTP:phosphocholine cytidylyltransferase; CDP-DAG, CDP-diacylglycerol; CDS, CDP-diacylglycerol synthase; VZ, ventricular zone; SVZ, subventricular zone; IZ, intermediate zone; E, embryonic day; WB, Western blotting; RT, room temperature; PTA, phosphotungstic acid; IF, immunofluorescence; DAPI, 4′,6-diamino-2-phenylindole, dihydrochloride; NA, numerical aperture; ANOVA, analysis of variance; CP, cortical plate.

References

1. Hatten, M. E. (1999) Expansion of CNS precursor pools: a new role for Sonic Hedgehog. *Neuron* **22,** 2–3 CrossRef Medline
2. Hatten, M. E. (1999) Central nervous system neuronal migration. *Annu. Rev. Neurosci.* **22,** 511–539 CrossRef Medline
3. Millet, L. J., and Gillette, M. U. (2012) Over a century of neuron culture: from the hanging drop to microfluidic devices. *Yale J. Biol. Med.* **85,** 501–521 Medline
4. Spillane, M., and Gallo, G. (2014) Involvement of Rho-family GTPases in axon branching. *Small GTPases* **5,** e27974 CrossRef Medline
5. Winkle, C. C., and Gupton, S. L. (2016) Membrane trafficking in neuronal development: ins and outs of neural connectivity. *Int. Rev. Cell Mol. Biol.* **322,** 247–280 CrossRef Medline
6. Cáceres, A., Ye, B., and Dotti, C. G. (2012) Neuronal polarity: demarcation, growth and commitment. *Curr. Opin. Cell Biol.* **24,** 547–553 CrossRef Medline
7. Dotti, C. G., Sullivan, C. A., and Banker, G. A. (1988) The establishment of polarity by hippocampal neurons in culture. *J. Neurosci.* **8,** 1454–1468 CrossRef Medline
8. Schelski, M., and Bradke, F. (2017) Neuronal polarization: from spatiotemporal signaling to cytoskeletal dynamics. *Mol. Cell. Neurosci.* **84,** 11–28 CrossRef Medline
9. Armijo-Weingart, L., and Gallo, G. (2017) It takes a village to raise a branch: cellular mechanisms of the initiation of axon collateral branches. *Mol. Cell. Neurosci.* **84,** 36–47 CrossRef Medline
10. Bullmore, E., and Sporns, O. (2012) The economy of brain network organization. *Nat. Rev. Neurosci.* **13,** 336–349 CrossRef Medline
11. Tracey, T. J., Steyn, F. J., Wolvetang, E. J., and Ngo, S. T. (2018) Neuronal lipid metabolism: multiple pathways driving functional outcomes in health and disease. *Front. Mol. Neurosci.* **11,** 10 CrossRef Medline
12. Quiroga, S., Bisbal, M., and Cáceres, A. (2018) Regulation of plasma membrane expansion during axon formation. *Dev. Neurobiol.* **78,** 170–180 CrossRef Medline
13. Pfenninger, K. H. (2009) Plasma membrane expansion: a neuron's Herculean task. *Nat. Rev. Neurosci.* **10,** 251–261 CrossRef Medline
14. Vance, J. E., Campenot, R. B., and Vance, D. E. (2000) The synthesis and transport of lipids for axonal growth and nerve regeneration. *Biochim. Biophys. Acta* **1486,** 84–96 CrossRef Medline
15. Tsukita, S., and Ishikawa, H. (1976) Three-dimensional distribution of smooth endoplasmic reticulum in myelinated axons. *J. Electron Microsc. (Tokyo)* **25,** 141–149 CrossRef Medline
16. Gonzalez, C., and Couve, A. (2014) The axonal endoplasmic reticulum and protein trafficking: cellular bootlegging south of the soma. *Semin. Cell Dev. Biol.* **27,** 23–31 CrossRef Medline

17. Luarte, A., Cornejo, V. H., Bertin, F., Gallardo, J., and Couve, A. (2018) The axonal endoplasmic reticulum: one organelle-many functions in development, maintenance, and plasticity. *Dev. Neurobiol.* **78,** 181–208 CrossRef Medline
18. Vance, J. E., Pan, D., Vance, D. E., and Campenot, R. B. (1991) Biosynthesis of membrane lipids in rat axons. *J. Cell Biol.* **115,** 1061–1068 CrossRef Medline
19. Vance, J. E., Pan, D., Campenot, R. B., Bussière, M., and Vance, D. E. (1994) Evidence that the major membrane lipids, except cholesterol, are made in axons of cultured rat sympathetic neurons. *J. Neurochem.* **62,** 329–337 CrossRef Medline
20. Posse de Chaves, E., Vance, D. E., Campenot, R. B., and Vance, J. E. (1995) Axonal synthesis of phosphatidylcholine is required for normal axonal growth in rat sympathetic neurons. *J. Cell Biol.* **128,** 913–918 CrossRef Medline
21. Curran, T., and Morgan, J. I. (1987) Memories of Fos. *Bioessays* **7,** 255–258 CrossRef Medline
22. Hughes, P., and Dragunow, M. (1995) Induction of immediate-early genes and the control of neurotransmitter-regulated gene expression within the nervous system. *Pharmacol. Rev.* **47,** 133–178 Medline
23. Caputto, B. L., and Guido, M. E. (2000) Immediate early gene expression within the visual system: light and circadian regulation in the retina and the suprachiasmatic nucleus. *Neurochem. Res.* **25,** 153–162 CrossRef Medline
24. Angel, P., and Karin, M. (1991) The role of Jun, Fos and the AP-1 complex in cell-proliferation and transformation. *Biochim. Biophys. Acta* **1072,** 129–157 CrossRef Medline
25. Guido, M. E., de Arriba Zerpa, G. A., Bussolino, D. F., and Caputto, B. L. (1996) Immediate early gene c-*fos* regulates the synthesis of phospholipids but not of gangliosides. *J. Neurosci. Res.* **43,** 93–98 CrossRef Medline
26. Bussolino, D. F., de Arriba Zerpa, G. A., Grabois, V. R., Conde, C. B., Guido, M. E., and Caputto, B. L. (1998) Light affects c-*fos* expression and phospholipid synthesis in both retinal ganglion cells and photoreceptor cells in an opposite way for each cell type. *Brain Res. Mol. Brain Res.* **58,** 10–15 CrossRef Medline
27. de Arriba Zerpa, G. A., Guido, M. E., Bussolino, D. F., Pasquare, S. J., Castagnet, P. I., Giusto, N. M., and Caputto, B. L. (1999) Light exposure activates retina ganglion cell lysophosphatidic acid acyl transferase and phosphatidic acid phosphatase by a c-Fos-dependent mechanism. *J. Neurochem.* **73,** 1228–1235 CrossRef Medline
28. Bussolino, D. F., Guido, M. E., Gil, G. A., Borioli, G. A., Renner, M. L., Grabois, V. R., Conde, C. B., and Caputto, B. L. (2001) c-Fos associates with the endoplasmic reticulum and activates phospholipid metabolism. *FASEB J.* **15,** 556–558 CrossRef Medline
29. Alfonso Pecchio, A. R., Cardozo Gizzi, A. M., Renner, M. L., Molina-Calavita, M., and Caputto, B. L. (2011) c-Fos activates and physically interacts with specific enzymes of the pathway of synthesis of polyphosphoinositides. *Mol. Biol. Cell* **22,** 4716–4725 CrossRef Medline
30. Gil, G. A., Silvestre, D. C., Tomasini, N., Bussolino, D. F., and Caputto, B. L. (2012) Controlling cytoplasmic c-Fos controls tumor growth in the peripheral and central nervous system. *Neurochem. Res.* **37,** 1364–1371 CrossRef Medline
31. Cardozo Gizzi, A. M., Prucca, C. G., Gaveglio, V. L., Renner, M. L., Pasquaré, S. J., and Caputto, B. L. (2015) The catalytic efficiency of lipin 1β increases by physically interacting with the proto-oncoprotein c-Fos. *J. Biol. Chem.* **290,** 29578–29592 CrossRef Medline
32. Gil, G. A., Bussolino, D. F., Portal, M. M., Alfonso Pecchio, A., Renner, M. L., Borioli, G. A., Guido, M. E., and Caputto, B. L. (2004) c-Fos activated phospholipid synthesis is required for neurite elongation in differentiating PC12 cells. *Mol. Biol. Cell* **15,** 1881–1894 CrossRef Medline
33. Dragunow, M., Peterson, M. R., and Robertson, H. A. (1987) Presence of c-fos-like immunoreactivity in the adult rat brain. *Eur. J. Pharmacol.* **135,** 113–114 CrossRef Medline
34. Dragunow, M., and Robertson, H. A. (1987) Generalized seizures induce c-fos protein(s) in mammalian neurons. *Neurosci. Lett.* **82,** 157–161 CrossRef Medline
35. Silvestre, D. C., Maccioni, H. J., and Caputto, B. L. (2009) Content of endoplasmic reticulum and Golgi complex membranes positively correlates with the proliferative status of brain cells. *J. Neurosci. Res.* **87,** 857–865 CrossRef Medline
36. Gordon, G. W., Berry, G., Liang, X. H., Levine, B., and Herman, B. (1998) Quantitative fluorescence resonance energy transfer measurements using fluorescence microscopy. *Biophys. J.* **74,** 2702–2713 CrossRef Medline
37. Lykidis, A., Jackson, P. D., Rock, C. O., and Jackowski, S. (1997) The role of CDP-diacylglycerol synthetase and phosphatidylinositol synthase activity levels in the regulation of cellular phosphatidylinositol content. *J. Biol. Chem.* **272,** 33402–33409 CrossRef Medline
38. Racca, A. C., Prucca, C. G., and Caputto, B. L. (2019) Fra-1 and c-Fos N-terminal deletion mutants impair breast tumor cell proliferation by blocking lipid synthesis activation. *Front. Oncol.* **9,** 544 CrossRef Medline
39. Galliard, T., Michell, R. H., and Hawthorne, J. N. (1965) Incorporation of phosphate into diphosphoinositide by subcellular fractions from liver. *Biochim. Biophys. Acta* **106,** 551–563 CrossRef Medline
40. Hayashi, K., Yagihara, Y., Nakamura, I., Katagiri, A., Arakawa, Y., and Yamazoe, S. (1967) Incorporation of ^{32}P from [γ-^{32}P]ATP into polyphosphoinositides and phosphatidic acid in subcellular particles of guinea pig brain. *J. Biochem.* **62,** 15–20 CrossRef Medline
41. Schibeci, A., and Schacht, J. (1977) Action of neomycin on the metabolism of polyphosphoinositides in the guinea pig kidney. *Biochem. Pharmacol.* **26,** 1769–1774 CrossRef Medline
42. Sun, G. Y., and Lin, T. N. (1989) Time course for labeling of brain membrane phosphoinositides and other phospholipids after intracerebral injection of [^{32}P]ATP. Evaluation by an improved HPTLC procedure. *Life Sci.* **44,** 689–696 CrossRef Medline
43. Wissing, J. B., and Behrbohm, H. (1993) Diacylglycerol pyrophosphate, a novel phospholipid compound. *FEBS Lett.* **315,** 95–99 CrossRef Medline
44. Tong, W., and Sun, G. Y. (1994) Phosphorylation of lipids in rat primary glial cells and immortalized astrocytes (DITNC). *Lipids* **29,** 385–390 CrossRef Medline
45. Ferrero, G. O., Renner, M. L., Gil, G. A., Rodríguez-Berdini, L., and Caputto, B. L. (2014) c-Fos-activated synthesis of nuclear phosphatidylinositol 4,5-bisphosphate [PtdIns(4,5)P(2)] promotes global transcriptional changes. *Biochem. J.* **461,** 521–530 CrossRef Medline
46. Kwan, A. C., and Dan, Y. (2012) Dissection of cortical microcircuits by single-neuron stimulation *in vivo*. *Curr. Biol.* **22,** 1459–1467 CrossRef Medline
47. Tabata, H., and Nakajima, K. (2003) Multipolar migration: the third mode of radial neuronal migration in the developing cerebral cortex. *J. Neurosci.* **23,** 9996–10001 CrossRef Medline
48. Bielas, S., Higginbotham, H., Koizumi, H., Tanaka, T., and Gleeson, J. G. (2004) Cortical neuronal migration mutants suggest separate but intersecting pathways. *Annu. Rev. Cell Dev. Biol.* **20,** 593–618 CrossRef Medline
49. Noctor, S. C., Martínez-Cerdeno, V., Ivic, L., and Kriegstein, A. R. (2004) Cortical neurons arise in symmetric and asymmetric division zones and migrate through specific phases. *Nat. Neurosci.* **7,** 136–144 CrossRef Medline
50. Nadarajah, B., and Parnavelas, J. G. (2002) Modes of neuronal migration in the developing cerebral cortex. *Nat. Rev. Neurosci.* **3,** 423–432 CrossRef Medline
51. Stipursky, J., Francis, D., and Gomes, F. C. (2012) Activation of MAPK/PI3K/SMAD pathways by TGF-β_1 controls differentiation of radial glia into astrocytes *in vitro*. *Dev. Neurosci.* **34,** 68–81 CrossRef Medline
52. Weiss, P., and Hiscoe, H. B. (1948) Experiments on the mechanism of nerve growth. *J. Exp. Zool.* **107,** 315–395 CrossRef Medline
53. Ledeen, R. W. (1985) *Transport, Exchange, and Transfer of Phospholipids in the Nervous System*, pp. 135–172, John Wiley & Sons, Inc., New York
54. Palay, S. L. (1958) The morphology of synapses in the central nervous system. *Exp. Cell Res.* **14,** 275–293 Medline
55. Droz, B., Rambourg, A., and Koenig, H. L. (1975) The smooth endoplasmic reticulum: structure and role in the renewal of axonal membrane and synaptic vesicles by fast axonal transport. *Brain Res.* **93,** 1–13 CrossRef Medline
56. Rambourg, A., and Droz, B. (1980) Smooth endoplasmic reticulum and axonal transport. *J. Neurochem.* **35,** 16–25 CrossRef Medline

57. Broadwell, R. D., and Cataldo, A. M. (1983) The neuronal endoplasmic reticulum: its cytochemistry and contribution to the endomembrane system. I. Cell bodies and dendrites. *J. Histochem. Cytochem.* **31,** 1077–1088 CrossRef Medline
58. Lindsey, J. D., and Ellisman, M. H. (1985) The neuronal endomembrane system. III. The origins of the axoplasmic reticulum and discrete axonal cisternae at the axon hillock. *J. Neurosci.* **5,** 3135–3144 CrossRef Medline
59. Willis, D., Li, K. W., Zheng, J. Q., Chang, J. H., Smit, A. B., Kelly, T., Merianda, T. T., Sylvester, J., van Minnen, J., and Twiss, J. L. (2005) Differential transport and local translation of cytoskeletal, injury-response, and neurodegeneration protein mRNAs in axons. *J. Neurosci.* **25,** 778–791 CrossRef Medline
60. Valenzuela, J. I., Jaureguiberry-Bravo, M., and Couve, A. (2011) Neuronal protein trafficking: emerging consequences of endoplasmic reticulum dynamics. *Mol. Cell. Neurosci.* **48,** 269–277 CrossRef Medline
61. Merianda, T., and Twiss, J. (2013) Peripheral nerve axons contain machinery for co-translational secretion of axonally-generated proteins. *Neurosci. Bull.* **29,** 493–500 CrossRef Medline
62. Rao, K., Stone, M. C., Weiner, A. T., Gheres, K. W., Zhou, C., Deitcher, D. L., Levitan, E. S., and Rolls, M. M. (2016) Spastin, atlastin, and ER relocalization are involved in axon but not dendrite regeneration. *Mol. Biol. Cell* **27,** 3245–3256 CrossRef Medline
63. Kumara-Siri, M. H., and Gould, R. M. (1980) Enzymes of phospholipid synthesis: axonal *versus* Schwann cell distribution. *Brain Res.* **186,** 315–330 CrossRef Medline
64. Gould, R. M., Pant, H., Gainer, H., and Tytell, M. (1983) Phospholipid synthesis in the squid giant axon: incorporation of lipid precursors. *J. Neurochem.* **40,** 1293–1299 CrossRef Medline
65. Gould, R. M., Spivack, W. D., Robertson, D., and Poznansky, M. J. (1983) Phospholipid synthesis in the squid giant axon: enzymes of phosphatidylinositol metabolism. *J. Neurochem.* **40,** 1300–1306 CrossRef Medline
66. Tanaka, T., Yamaguchi, H., Kishimoto, Y., and Gould, R. M. (1987) Lipid metabolism in various regions of squid giant nerve fiber. *Biochim. Biophys. Acta* **922,** 85–94 CrossRef Medline
67. Caubet, J. F. (1989) c-fos proto-oncogene expression in the nervous system during mouse development. *Mol. Cellular Biol.* **9,** 2269–2272 CrossRef Medline
68. Gallo, F. T., Katche, C., Morici, J. F., Medina, J. H., and Weisstaub, N. V. (2018) Immediate Early genes, memory and psychiatric disorders: focus on c-Fos, Egr1 and Arc. *Front. Behav. Neurosci.* **12,** 79 CrossRef Medline
69. Velazquez, F. N., Prucca, C. G., Etienne, O., D'Astolfo, D. S., Silvestre, D. C., Boussin, F. D., and Caputto, B. L. (2015) Brain development is impaired in c-*fos* -/- mice. *Oncotarget* **6,** 16883–16901 CrossRef Medline
70. Morgan, J. I., and Curran, T. (1988) Calcium as a modulator of the immediate-early gene cascade in neurons. *Cell Calcium* **9,** 303–311 CrossRef Medline
71. Sagar, S. M., Sharp, F. R., and Curran, T. (1988) Expression of c-fos protein in brain: metabolic mapping at the cellular level. *Science* **240,** 1328–1331 CrossRef
72. Banker, G. A., and Cowan, W. M. (1977) Rat hippocampal neurons in dispersed cell culture. *Brain Res.* **126,** 397–425 CrossRef Medline
73. Borioli, G. A., Caputto, B. L., and Maggio, B. (2001) c-Fos is surface active and interacts differentially with phospholipid monolayers. *Biochem. Biophys. Res. Commun.* **280,** 9–13 CrossRef Medline
74. Ferrero, G. O., Velazquez, F. N., and Caputto, B. L. (2012) The kinase c-Src and the phosphatase TC45 coordinately regulate c-Fos tyrosine phosphorylation and c-Fos phospholipid synthesis activation capacity. *Oncogene* **31,** 3381–3391 CrossRef Medline
75. Portal, M. M., Ferrero, G. O., and Caputto, B. L. (2007) N-terminal c-Fos tyrosine phosphorylation regulates c-Fos/ER association and c-Fos-dependent phospholipid synthesis activation. *Oncogene* **26,** 3551–3558 CrossRef Medline
76. Rodriguez-Berdini, L., and Ferrero, G. O. (2016) A technique for the measurement of *in vitro* phospholipid synthesis via radioactive labeling. *Bio-protocol* **6** CrossRef
77. Saito, T., and Nakatsuji, N. (2001) Efficient gene transfer into the embryonic mouse brain using *in vivo* electroporation. *Dev. Biol.* **240,** 237–246 CrossRef Medline